Spectrochimica Acta Part A: Molecular and Biomolecular Spectroscopy 146 (2015) 142–150

Contents lists available at ScienceDirect

Spectrochimica Acta Part A: Molecular and Biomolecular Spectroscopy

journal homepage: www.elsevier.com/locate/saa

Three novel input logic gates supported by fluorescence studies: Organic nanoparticles (ONPs) as chemo-sensor for detection of Zn^{2+} and Al^{3+} in aqueous medium

C.A. Huerta-Aguilar [a], T. Pandiyan [a,*], N. Singh [b], N. Jayanthi [c]

[a] *Facultad de Química, Universidad Nacional Autónoma de México (UNAM), Ciudad Universitaria, Coyoacán 04510, México D.F., Mexico*
[b] *Indian Institute of Technology (IIT), Ropar, Punjab, India*
[c] *División de Nanotecnología, Universidad Politécnica del Valle de México (UPVM), Av. Mexiquense, C.P. 54910 Tultitlan, Estado de México, Mexico*

HIGHLIGHTS

- Three novel input logic gates supported by fluorescence studies.
- Organic nanoparticles as chemo-sensor for detection of Zn^{2+}.
- pH and temperature influence on the fluorescence in the detection of Zn^{2+}.

GRAPHICAL ABSTRACT

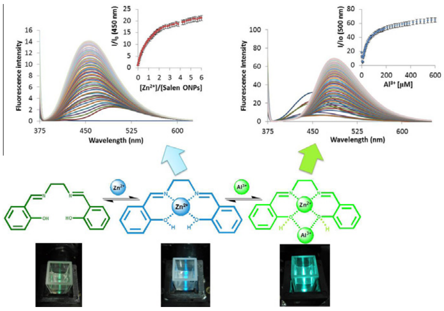

ARTICLE INFO

Article history:
Received 29 October 2014
Received in revised form 10 February 2015
Accepted 6 March 2015
Available online 12 March 2015

Keywords:
Organic nanoparticles (ONPs)
Logic gates
Recognition of Zn^{2+}
Fluorescence studies

ABSTRACT

Organic nanoparticles (ONPs) of N,N′-ethylenebis(salicylimine) (salen) were synthesized and applied for specific recognition of Zn^{2+} and Al^{3+} ions in an aqueous medium. The results show that fluorescence intensity rises with the increasing concentration of Zn^{2+} in salen solution, proving that salen-ONPs detect Zn^{2+} efficiently in the aqueous medium as chemo-sensor. Furthermore, the salen-ONPs/Zn^{2+} system performs as an ON–OFF switch between pH 6.0 and 4.0. Amusingly, although salen-ONPs/Al^{3+} does not show any significant effect in the fluorescence spectra, highest fluorescence intensity was observed when Al^{3+} ion was added to salen-ONPs/Zn^{2+} in a sequential order (addition of Zn^{2+} to salen-ONPs, followed by Al^{3+}). This system can be applied as a novel three inputs logic gate supported by the fluorescence for the detection of Zn^{2+} and Al^{3+} in biological and environmental samples. It appears that photo induced electron transfer (PET) occurs in the salen-ONPs when the fluorophore is excited. For salen/Zn^{2+} system, the PET is being inhibited considerably by lowering the receptor HOMO energy due to the formation of a bond between the metal ion and ligand, enhancing the fluorescence emission. This is consistent with the theoretical study that the energy of HOMO of the ligand is lower than that of $Zn(salen)^{2+}$ complex.

Introduction

New materials that exhibit electronic, magnetic and optical properties are currently of great interest in the development of molecular devices because they mimic or mirror the action of macroscopic tools such as switches, motors and other machinery [1–4]; moreover, the change of modes (OFF and ON) in those properties can be modulated by employing external inputs such as ions, molecules, light etc [5–10]. Luminescence, one of most useful techniques, is being considered to monitor the molecular level functions; for example, in DNA-based logic gates, fluorescent signals

---

[*] Corresponding author. Tel.: +52 55 56223499.
E-mail address: pandiyan@servidor.unam.mx (T. Pandiyan).

http://dx.doi.org/10.1016/j.saa.2015.03.082
1386-1425/

are developed with respect to chemical reactions generated by ions, light or molecules as inputs in the Boolean operations [11–15]. Thus molecular logic gates [16,9,17–22] were used for biochemical optical sensors [23] or semiconductor QD [24–27]. In the studies, mostly, metal based nanoparticles (NPs) have been used as fluorescent biological labels [28–30], light-emitting diodes (LEDs) [31], and optical sensors [32,33].

Organic molecules hetero atoms or bio-molecules such DNA chains have been employed as surface capping agents for metal NPs in order to prevent NPs aggregation [34–39] and also for achieving bio-compatibility. Nevertheless, the studies of organic molecules in the concept of NPs and also the development of molecular logic gate based on Organic nanoparticles (ONP) are very limited in the literature when compared to metal NPs [40–43]. The electronic and optical properties of organic molecular crystals are fundamentally different from those of inorganic metals or semiconductors due to the presence of weak intermolecular interaction forces (van der Waals type) [44]. For example, in organic nanoparticles studies, the size dependent fluorescent properties of perylene, pyrazoline and phthalocyanine have been established [45–47]. Thus the electronic/optical behaviors of ONPs are expected to be interesting because of their variability and flexibility.

Numerous chemical and biochemical analytes can be detected by fluorescence methods: cations (H^+, Li^+, Na^+, Ca^{2+}, Mg^{2+} Zn^{2+}, Pb^{2+}, Cd^{2+}, Al^{2+}, Cr^{3+}, etc.), and anions (halides, citrates, carboxylates, phosphates, etc.), neutral molecules (sugars e.g., glucose). The development of these types of chemo-sensors is of major importance for simultaneous detection of Zn^{2+} and Al^{3+} ions in environmental and biological systems at very low concentrations. Generally, Zn^{2+} is commonly present in environment and biological systems, the detection of this ion becomes vital, and the presence of aluminum ion can be used as indicator of some metabolic malfunctions.

Conjugate-schiff base ligands are being considered for chemosensors [48] because the C═N structure (π acceptors) is generally non-fluorescent and becomes fluorescent when the schiff base is adequately modified. For instance, the addition of aromatic structure to the schiff base is such that the isomerization of C═N structure is inhibited to change the fluorescence behavior [49]. Only a few reports on the ONP of Schiff bases are present in the literature [50–52]; moreover, the application of these ONPs in developing a logic gate system is unexplored. In the present work, the ONPs of N,N′-ethylenebis(salicylimine) (salen) is chosen to detect metal ions through the function of logic gates. In particular, the specific detection of Zn^{2+} ions in aqueous medium is important as it plays a key role in human metabolism and also in synaptic plasticity [53,54]. The present study shows that salen-ONPs detect Zn^{2+} efficiently in aqueous medium and acts as a chemo-sensor, performing a novel input logic gate supported by fluorescence, which increases the intensity many fold in the presence of Al^{3+} ions.

Experimental section

Materials and methods

All chemicals for the preparation of salen ligand were used as received from Sigma-Aldrich and THF (J.T. Baker) was used in the synthesis of salen-ONPs.

Physical measurements

Elemental analyses were carried out on a Fisons (Model EA 1108 CHNSO). NMR (300 MHz Varian) and Mass Spectrometry (LECO Pegasus 4D) with a TOF analyzer were used to characterize the ligand. To determine the size and composition of ONPs, Transmission Electron Microscope (TEM, JEOL JEM 2010) equipped with Energy Dispersive and X-Ray Spectroscopy micro-analyzer ((EDS, Oxford ISIS) was used. UV–Vis spectrophotometer (Perkin-Elmer Lambda 25) and fluorescence spectrophotometer (F-96 Pro) were employed to analyze electronic and fluorescence properties of salen-ONP as well as for the detection of metal ions.

Preparation of ligand N,N′-ethylenebis(salicylimine)) (salen)

Salen was prepared as reported elsewhere [55]: To solution of 2-hydroxybenzaldehyde (2.0 mmol) dissolved in ethanol (30 mL), ethylenediamine (1.0 mmol) was added, and then the resulting solution was stirred for 30 min at 40 °C to yield a yellow product, which was filtered and dried in vacuum (Scheme 1).

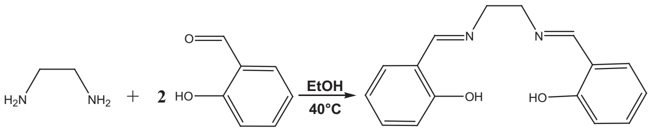

Synthesis of Ligand 1 (salen)

Yield, 88.95%. Elemental analysis for $C_{16}H_{16}O_2N_2$: Calcd.: C, 71.62; H, 6.01; N, 10.44. Found, C, 71.94; H, 5.64; N, 10.85. ^1H NMR (300 MHz, CD3OD) δ (ppm): 3.94 (s, 2H, ethylenediamine), 6.82 (t, 2H, phenyl ring), 6.84 (s, 2H, phenyl ring), 7.25 (d, 2H, phenyl ring), 7.30 (m, 2H, phenyl ring), 8.44 (s, 2H, R–N═C–R).

Preparation of organic nanoparticles

The preparation of salen-ONPs is followed as reported previously [56]: salen ligand (14.5 mg, 0.05 mmol) is first dissolved in tetrahydrofuran (1.0 ml), then it was injected slowly into deionized water (100 ml) under sonication. The resulting mixture was further sonicated for 15 min. to yield a colloidal suspension of salen-ONP (0.5 mM) and they were characterized by TEM and EDX analyses [57].

Results and discussion

The nature of salen-ONPs was analyzed by TEM and EDX, showing that the sphere shaped small ONPs (2.0 nm) are uniformly formed (Fig. 1). In the EDX analysis, signals corresponding to C and O were observed, confirming the organic nature of the particles. Since the ONPs are generally volatile and are not stable under typical conditions of TEM analyses, they differ in the elemental composition of salen ONPs in the EDX.

Metal binding studies with salen-ONPs

The selective recognition of different metal ions (Mg^{2+}, Al^{3+}, Cr^{3+}, Mn^{2+}, Fe^{3+}, Ni^{2+}, Cu^{2+}, Zn^{2+}, Sr^{2+}, Sm^{3+}, Ag^+, and Cd^{2+} as nitrate salts) with salen-ONPs was analyzed by UV-visible and fluorescence techniques. The nanoparticles (NPs) of salen are insoluble (colloid nature) in water. The UV visible spectra of NPs of salen in methanol and also in water are recorded, and there has been no a change in the spectra in both solvents. This confirms that hydrolysis does not take place in the ligand in the water medium. Moreover, if the ligand undergoes hydrolysis, the fluorescence intensity is expected to decrease or disappear due to the loss of conjugation. In the experiment, each metal ion solution (50 μL, 0.1 mM) was added to salen-ONPs (3.0 mL of 0.15 mM) suspended in water, then the full UV–Vis spectra (200–800 nm), and the fluorescence emission (360–750 nm) were measured. In the UV–visible spectra, two peaks (250 and 330 nm) corresponding to the $-\pi^*$ and $\pi-\pi^*$ transitions were observed. In the fluorescence studies,

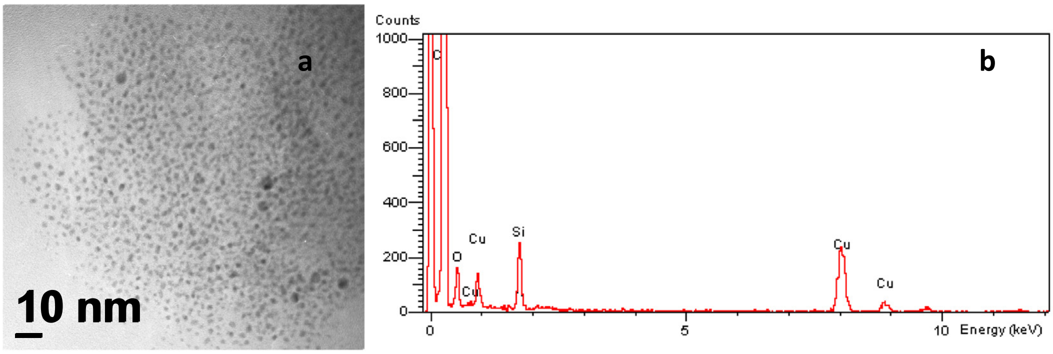

Fig. 1. Microscopic analysis of salen-ONPs: (a) TEM at 40,000 magnification; (b) EDX spectra.

salen-ONPs were exited at 365 nm and the corresponding fluorescent emission signal was observed at 490 nm.

In the fluorescence study, a high fluorescence response was observed for Zn^{2+} with respect to other cations, showing a specific recognition of Zn^{2+} ion when compare to other metal ions by salen-ONPs (see Fig. 2). In addition, there is a change in the fluorescent color from green to neon blue after addition of Zn^{2+} ions to salen-ONPs, shifting the wavelength from 490 to 450 nm. Furthermore, the salen-ONPs (0.15 mM) is able to detect Zn^{2+} ion even at low concentration (16.0 mM) in aqueous solution, and this detection threshold level is efficient to measure the concentration of Zn^{2+} in biological or environmental samples.

Titration studies of salen-ONPs against Zn^{2+} ions

The titration analysis was performed in order to prove the binding selectivity of salen-ONPs with Zn^{2+} ions. The florescent emission intensity was measured for each subsequent addition of Zn^{2+} ions (20.0–500.0 μM) to salen-ONPs (15.0 mM), and it was observed that the peak intensity increases with increasing concentration of Zn^{2+} in the ONPs (Fig. 3a). The intensity of fluorescence for salen-ONPs was also measured without Zn^{2+} ion. After analyzing the results, it was found that there is a good quasi-linear relationship between the intensity of fluorescent emission and the concentration of Zn^{2+} ion in the salen-ONPs (Fig. 3b), suggesting that salen-ONPs perform as chemo-sensors in recognizing Zn^{2+} in the aqueous solution. It appears that photo induced electron transfer (PET) occurs in the salen-ONPs when the fluorophore is excited. i.e., an electron is transferred from the HOMO (donor) to the low-lying HOMO of the acceptor (fluorophore), causing a low fluorescence emission. However, when Zn^{2+} is added to ONPs, metal ions involve in the binding with the salen moiety (recognition) and this causing the lowering of the receptor HOMO energy, thus inhibiting the photo-induced electron transfer from HOMO (donor) to fluorophore, and hence enhancing the fluorescence emission.

Stoichiometry determination of salen-ONPs against Zn^{2+}

Job's method was employed to determine the stoichiometry of the reaction between salen-ONPs and Zn^{2+} ions (Fig. 4). In the study, the fluorescence intensity increases proportionally up to ~2.0 equivalents during the addition of Zn^{2+} ions to ONPs at a ratio [Zn ion: salen-ONPs] of 2: 1; however, subsequently to this ratio, the proportionality decreased slightly to 6.0 equivalents (ratio: 6:1 for Zn ion:selen-ONPs). The detection limit was 20 μM for Zn^{2+} ion in aqueous medium, indicating that the binding proportionality of ligand with metal ion was not seen after ~2.0 equivalents. This is probably due to the nature of ONPs, where some of the molecules might be inside the particle, causing a low interaction with the metal ion.

Competitive binding analysis

The binding selectivity of salen-ONPs with Zn^{2+} was analyzed through fluorescence study in order to understand a possible interference of other metal ions. To the salen-ONPs (0.15 mM)/Zn^{2+} (16.0 mM), different metal ions (100.0 mM) were added in such a way that the final concentration is to be 16.0 mM. The resulting solution mixture was stirred for 15 min and kept for 5 min. to reach equilibrium, and then the fluorescence emission was measured in the visible region after excitation at 365 nm. The results show that there is a small interference from Cr^{3+}, Fe^{3+}, Co^{2+}, Ni^{2+} and Cu^{2+} ions during the recognition of Zn^{2+} through salen-ONPs

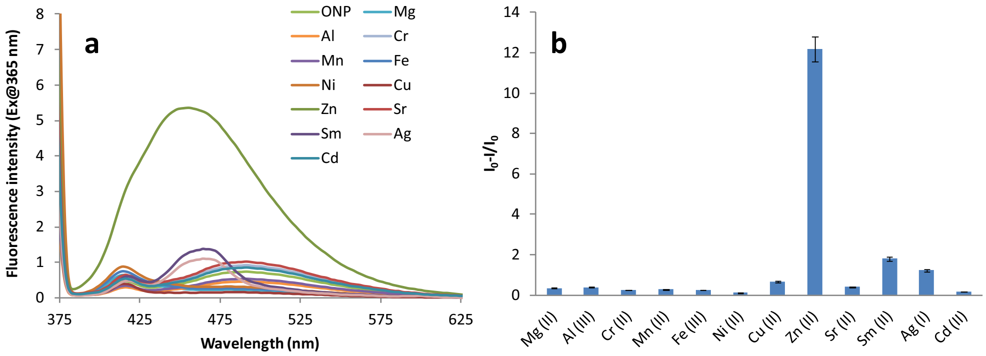

Fig. 2. Metal binding test of salen-ONPs with different metal ions: (a) Fluorescence spectra of salen-ONPs with respect to different cations; (b) Normalized fluorescence intensity for specific recognition of Zn^{2+} ions (50 μmol) at 450 nm.

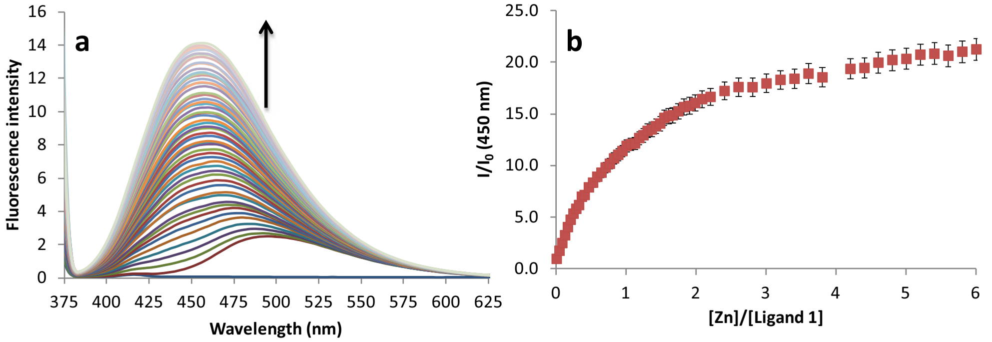

Fig. 3. Titration studies of salen-ONPs against Zn^{2+} ions: (a) the change of fluorescence intensity with respect to subsequent addition of Zn^{2+} ions (20–500 μM) to salen-ONPs; (b) quasi-linear relationship for (salen-ONPs vs. Zn^{2+}) and the fluorescence response with respect to the Zn^{2+} content in the solution.

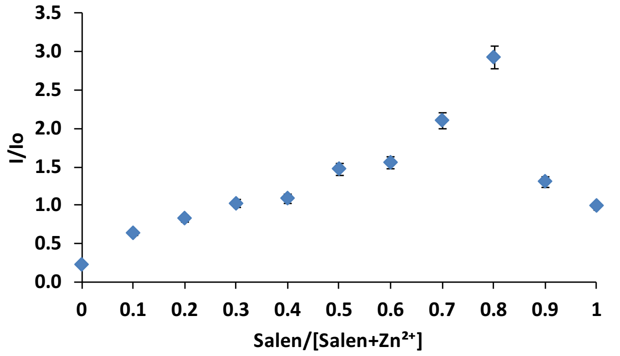

Fig. 4. Job's plot: stoichometry determination of Zn^{2+} with salen-ONPs.

(Fig. 5). It means that salen ligand can also bind with other metal ions owing to their similar chemical nature (ionic radius: Cr^{3+} (0.73 Å), Mn^{2+} (0.67 Å), Fe^{3+} (0.61 Å), Co^{2+} (0.65 Å), Ni^{2+} (0.69 Å), Cu^{2+} (0.73 Å) and Zn^{2+} (0.74 Å)). Moreover, the metal ions which have *d* orbitals can coordinate with salen in a similar manner and they can interfere with the fluorescence signal originated from Zn/ONPs. However, there is no considerable interference from Ag^+ (1.29 Å) or Cd^{2+} (1.09 Å) in the fluorescence because of their different acid-base chemistry.

Interestingly, although salen-ONPs/Al^{3+} does not show any significant effect in the fluorescence spectrum, an enhancement of fluorescence intensity was observed when Al^{3+} ion was added to salen-ONPs/Zn^{2+}. This indicates that Al^{3+} interacts efficiently with salen-ONPs/Zn^{2+} system in such a way that the fluorescence is highly magnified (Fig. 6), and this means that salen-ONPs/Zn^{2+}, which is an electronic conjugated fluorophore, has been further activated in the presence of Al^{3+} ion in the aqueous medium, increasing the intensity of fluorescence for [salen-ONPs/Zn^{2+}/Al^{3+}]. Furthermore, a quenching in the fluorescence intensity for [salen-ONPs/Zn^{2+}/Al^{3+}] was observed for the addition of the metal ions except for Sr^{2+}, Ag^+, Cd^{2+} and Mg^{2+}, and in addition, the fluorescence emission signal was slightly red shifted from 450 nm to 500 nm during the Al^{3+}addition to [salen-ONPs/Zn^{2+}].

To understand the binding of Al^{3+} ions with the [salen-ONPs/Zn^{2+}] system, the titration study was carried out by adding aliquots of $Al(NO_3)_3$ (100 mM) to the system (ratio: 2:1, salen-ONPs (15.0 mM))/Zn^{2+} (7.5 mM). The results show that the intensity of the characteristic peak (450 nm) of Zn^{2+}/ONPs was dramatically decreased, while growing a new peak around 500 nm during the addition of Al^{3+} (3.0–6.0 μM) to the [salen-ONPs/Zn^{2+}] system. The stoichiometry ratio of this system was determined by Job's method and was 1:2 for [salen-ONPs/Zn^{2+}]: Al^{3+} (Fig. 7).

For example, the fluorescence intensity (2.0 F.U.) measured for salen-ONPs (15.0 mM) at 500 nm increased to 16.2 for [salen-ONPs Zn^{2+}] (15.0 mM, 1:1 ratio) at 450 nm; interestingly, the intensity is further increased to 90 F.U. at 500 nm after addition of Al^{3+} solution to the system. For salen-ONPs-Zn^{2+} (15.0 mM)/Al^{3+} (0.6 mM) (1:1 ratio), a considerable increase in the florescence intensity was observed through Intramolecular photo-induced electron transfer (IPETS) [58]. For salen/Zn^{2+} system, the receptor HOMO energy is lowered when compared to salen-ONPs, and it inhibits PET from HOMO (donor) to fluorophore, enhancing the fluorescence emission. For the [salen/Zn^{2+}/Al^{3+}] system, the HOMO energy of the receptor is further stabilized in the presence

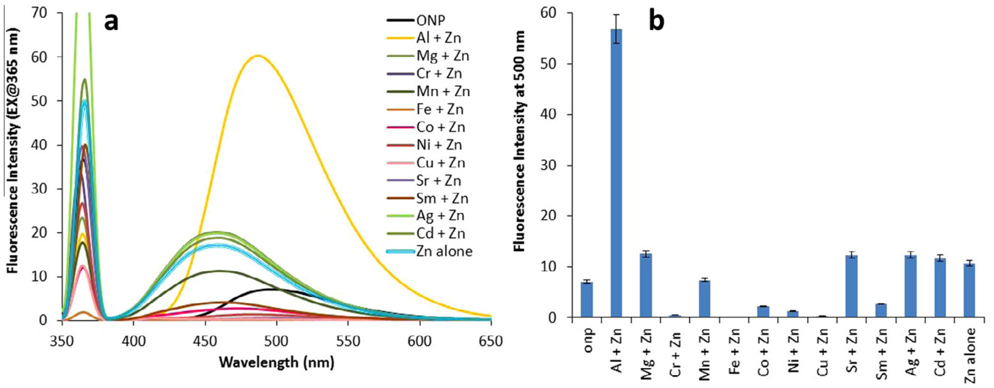

Fig. 5. (a) Competitive binding analysis of Zn^{2+}/salen-ONPs with different metal ions (Mg, Al^{3+}, Cr^{3+}, Mn^{2+}, Fe^{3+}, Co^{2+}, Ni^{2+}, Cu^{2+}, Sr^{2+}, Sm^{3+}, Ag^+ and Cd^{2+}) by fluorescence spectra. (b) Fluorescence intensity of competitive binding test for Zn^{2+} (16 mM) in the presence of other metal ions (16 mM) for salen-ONPs in aqueous solution.

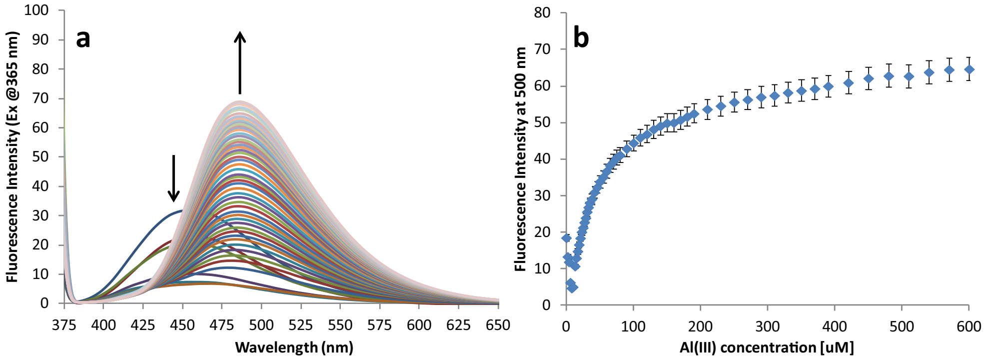

Fig. 6. Titration of [salen-ONPs/Zn^{2+}] against Al^{3+} ions: (a) the increase fluorescence intensity with the subsequent addition of Al^{3+} (2.0–600.0 μM); b) fluorescence response for the binding of [salen-ONPs/Zn^{2+}] with Al^{3+} ions.

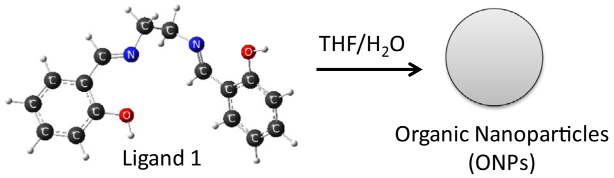

Scheme 1. Synthesis of salen-ONPs.

of Al^{3+}; besides the planarity of the complex structure is also increased, leading a strong PET from the receptor, and this enhances further the fluorescence emission (Scheme 2).

The interaction of Al^{3+} ions with Zn^{2+}/ligand is pH dependent. At high pH, high fluorescence intensity was observed, so there is a high possibility of deprotonation. Furthermore, the pHs were measured during addition of Al^{3+} ion to Zn^{2+}/salen system (suppl. Mat.), showing that pH was decreased with increasing concentration of Al^{3+} ion in Zn^{2+}/salen system.

Logic gate system salen-ONPs/Zn^{2+}/Al^{3+}

For salen-ONPs/Zn^{2+}, there exists a logic gate system in the presence of Al^{3+}, indicating that high fluorescence intensity takes place only when both Zn^{2+} and Al^{3+} are present in a sequential order; however, the intensity was low for other combinations of metal ions or in other sequential order. First, an AND logic gate performs through the binding of Zn^{2+} with salen-ONPs [A = 1, B = 1] (see suppl. Mat.), developing the fluorescence (at 450 nm). The intensity of the fluorescence has been further increased by complementary gate (other AND logic gate) in the presence of Al^{3+} ions. This means that the fluorescence intensity resulted from salen-ONPs/Zn^{2+} couple is further increased by adding another input (the presence of Al^{3+} ions), indicating that salen-ONPs first recognize Zn^{2+} ion, and then recognize Al^{3+}. The enhancement of fluorescence intensity occurs only when all inputs [A = 1, B = 1, C = 1] are given and it forms a three inputs AND logic gate system (Scheme 3). However, for other combinations with negative inputs [A = 0, B = 0 or C = 0], no fluorescence was found. This observation is consistent with other previous report [59].

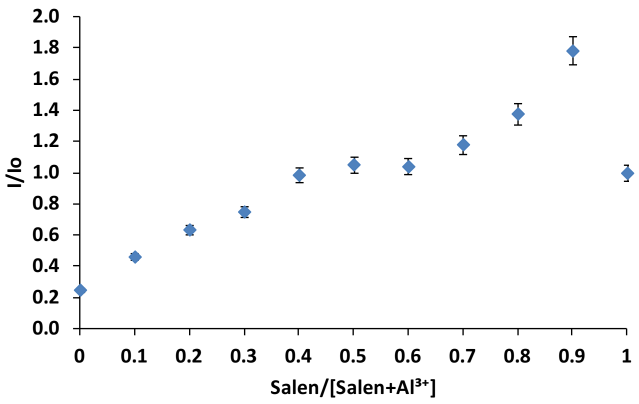

Fig. 7. Job's plot: determination of salen ONPs/Zn^{2+}/Al^{3+}.

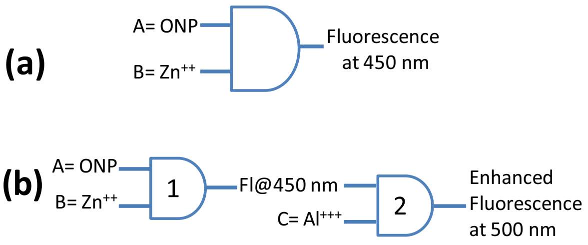

Effect of pH on the fluorescence intensity

The effect of pH on the fluorescence intensity for salen-ONPs was studied by adding HNO_3 (10.0 mM) or NH_3OH (10.0 mM). For each addition (acid or base), the intensity and the pH values were measured at excitation of 365 nm (Fig. 8). Similarly, for salen-ONPs/Zn^{2+} and also for salen-ONPs/Zn^{2+}/Al^{3+}, the same method was adopted. The results show that pH strongly influences the fluorescent emission. This observation agrees with other published works [60,61]. In the acidic condition (pH = 1.0–5.0), the fluorescence intensity was very low (OFF mode), and it becomes ON mode (enhancement of the fluorescence) at basic condition (pH = 6–10). The study shows that [ONPs/Zn^{2+}/Al^{3+}] exhibits a maximum intensity at pH 8.0. In the acid condition, photo-induced electron transfer in salen-receptor (fluorophore) is thermodynamically disallowed (switched-OFF), resulting in a low fluorescence owing to the protonation of imine amine nitrogens (C=N) in the receptor. While in the basic condition, the deprotonation is favored for the receptor, allowing the PET phenomenon, the system becomes switched-ON, exhibiting the fluorescence intensity. This shows that the salen ligand acts as ON–OFF sensor between pH 6.0 and pH 4.0.

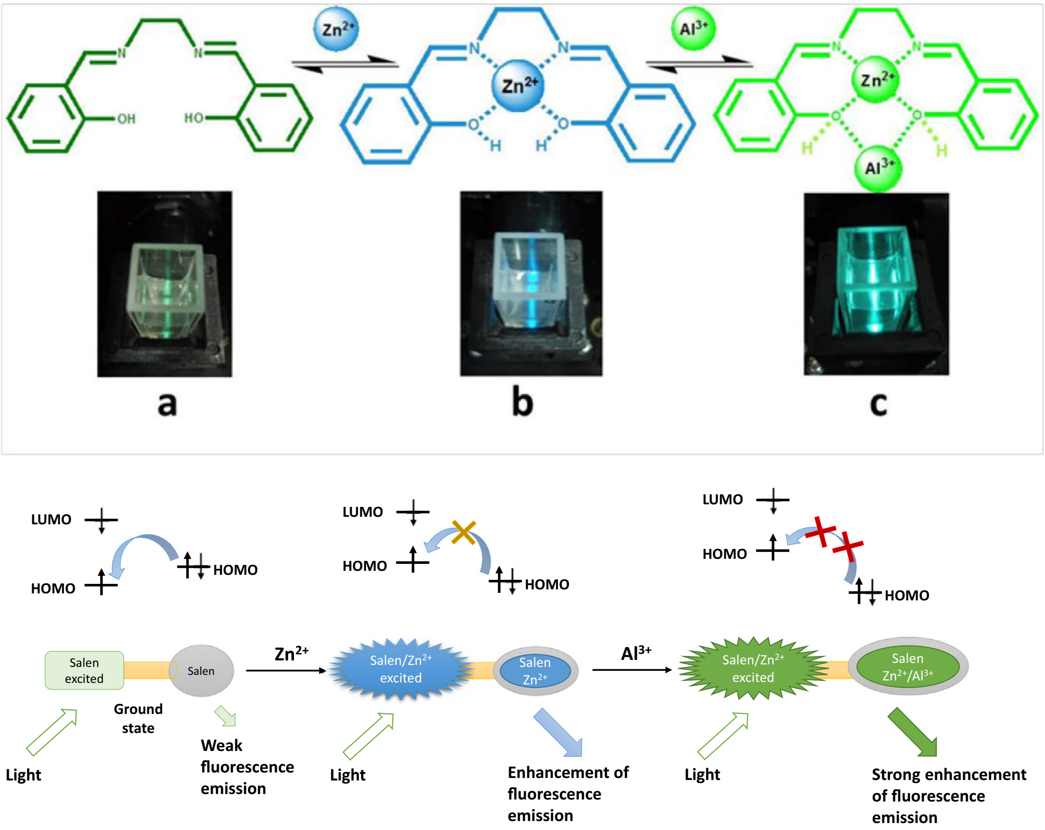

Scheme 2. The color change of fluorescence emission: (a) salen-ONPs = weak green; (b) Zn^{2+}/salen-ONPs (1:1 ratio) = neon blue, (c) Zn^{2+}/salen-ONPs/Al^{3+} = strong green fluorescence emission after addition of Al^{3+} ion (600 μM) to Zn^{2+}/salen-ONPs (2:1).

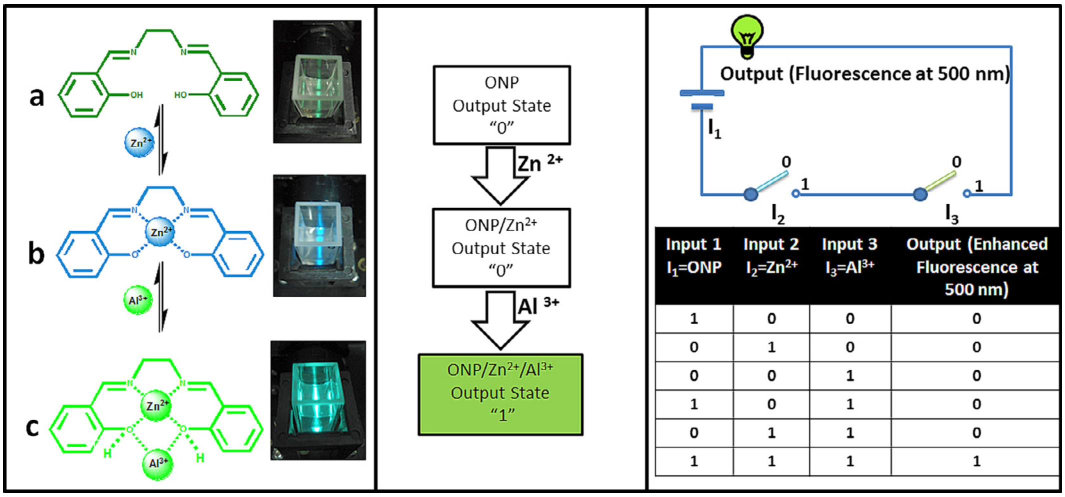

Input 1 I_1=ONP	Input 2 I_2=Zn^{2+}	Input 3 I_3=Al^{3+}	Output (Enhanced Fluorescence at 500 nm)
1	0	0	0
0	1	0	0
0	0	1	0
1	0	1	0
0	1	1	0
1	1	1	1

Scheme 3. Three inputs Logic Gate System: salen-ONPs with selective recognition of Zn^{2+} and Al^{3+} in aqueous solution. Three inputs are: 1 = ONPs, 2 = Zn^{2+} ion and 3 = Al^{3+} ion.

Temperature effect on fluorescence intensity

The effect of temperature (2.0–40 °C) on the fluorescence intensity was studied for all systems (salen-ONPs, salen-ONPs/Zn^{2+} and salen-ONPs/Zn^{2+}/Al^{3+}. The results show that a high fluorescence emission was observed when the temperature is low (see Suppl. Mat.), which is consistent with other studies [62–64]. For salen-ONPs, the fluorescence intensity was 8.5 F.U. at 2.0 °C, and the intensity was fluorescence quenched with increasing temperature. The same behavior was seen for all the systems although the magnitude of the emission differs for each system. This can be explained in that the thermal energy of the solution increases

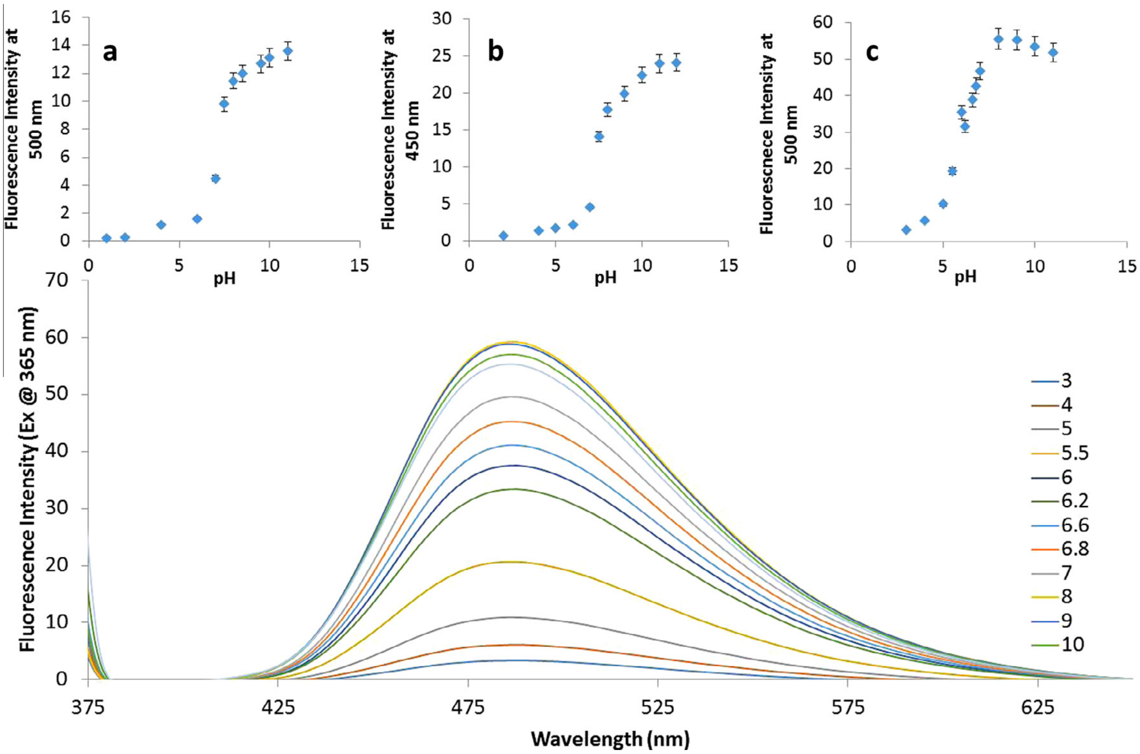

Fig. 8. pH effect (1.0–12) on the fluorescence intensity: (a) salen-ONPs, (b) salen-ONPs/Zn^{2+} and (c) salen-ONPs/Zn^{2+}/Al^{3+}.

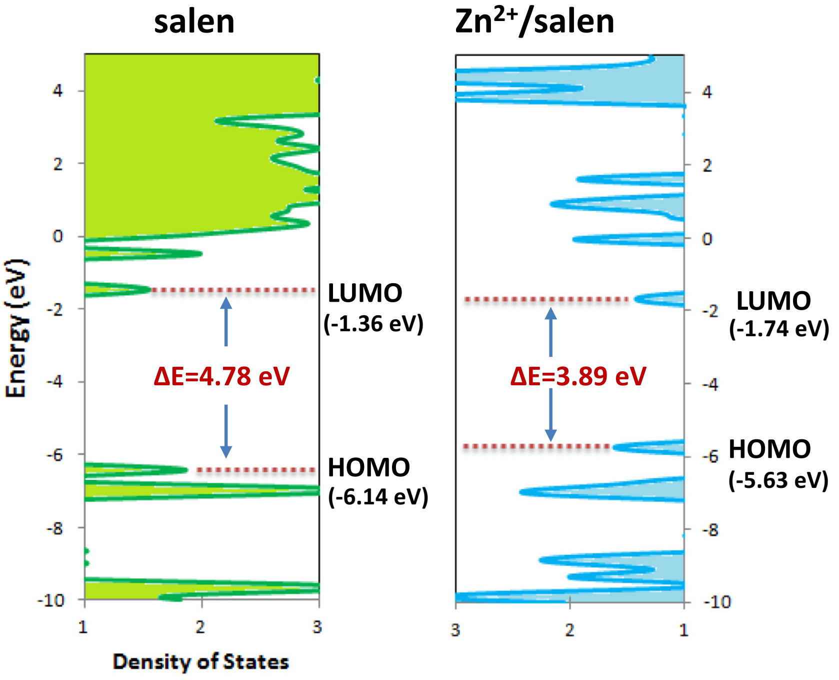

Fig. 9. Density of sates (electronic states) diagram: salen at B3LYP/6-311G(d,p) and $[Zn\text{-}salen]^{2+}$ at B3LYP/LANL2DZ/6-311G(d,p).

the electron moments between the molecules and so decreasing the intensity. In contrast, at low temperature, the intramolecular transference of electrons increases and so increases the fluorescent emission.

Computational procedure

For the salen-structure, the full optimization was performed by Density Functional Theory (DFT) using Gaussian'09 at B3LYP with 6-311+G(d,p) basis set [65], and Polarizable Continuum Mode (IEF-PCM) was used to see the solvent effect (water as solvent). The structural data obtained were used as input to calculate Time-Dependent DFT (TD-DFT) [66,67]. To optimize the structure of $[Zn\text{-}salen]^{2+}$, B3LYP with LANLDZ basis set was employed, and then UV–visible spectrum and Density of States (DOS) diagrams were obtained through TD-DFT calculations (Fig. 9).

In the structure, two nitrogen and two oxygen atoms are coordinated with Zn^{2+} ion due to their negative charge detected by the

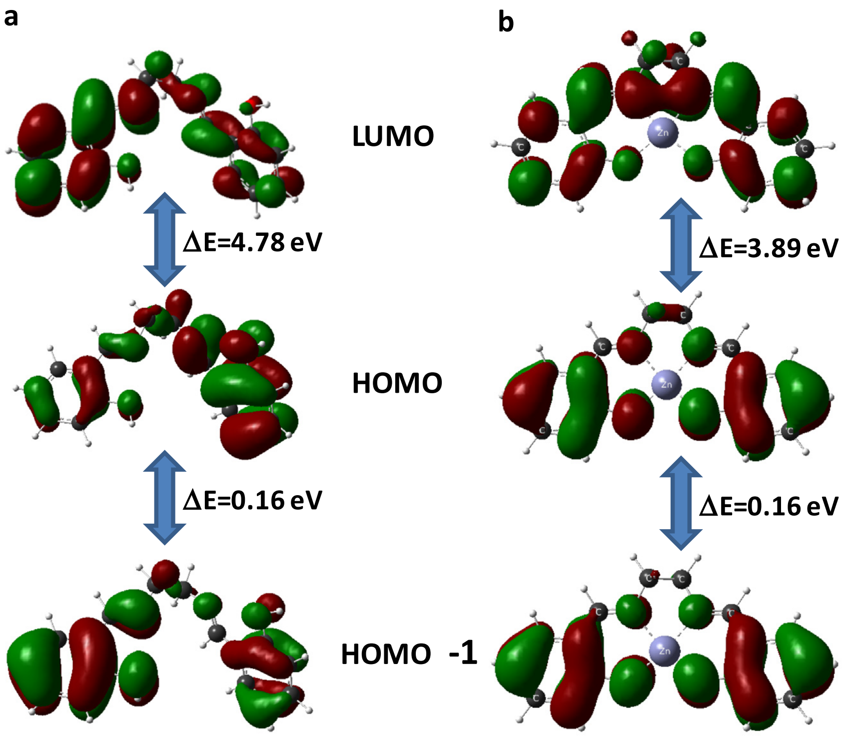

Fig. 10. Frontie molecular orbital (FMO) diagram for (a) salen (b) salen/Zn^{2+}.

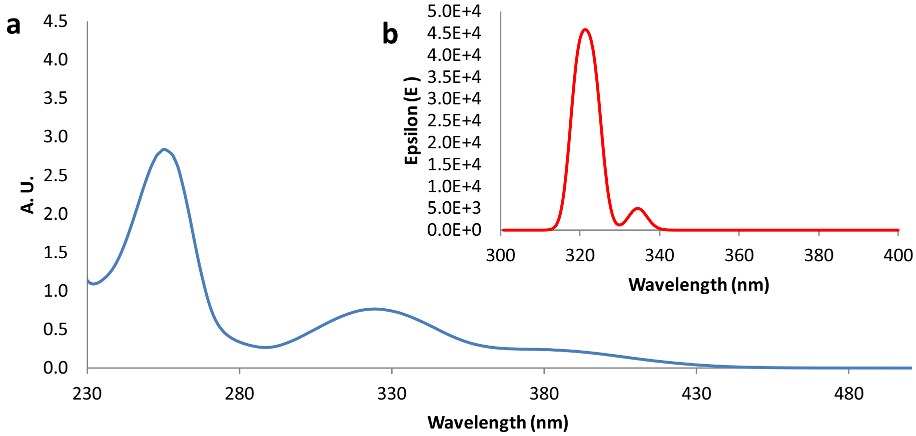

Fig. 11. UV–Vis spectra: (a) experimental spectra of salen in solvent mixture (THF: H_2O, 1:99); (b) TD-DFT spectra of the ligand at B3LYP/6-311G(d,p) in THF as solvent.

electrostatic potential analysis (Suppl. Mat.). It shows that the ligand (receptor) can coordinate efficiently with the metal ion (acceptor).

DOS diagram was derived for both the ligand and $[\text{Zn-salen}]^{2+}$ complex through Energy DFT technique, and the results show that for the ligand, the band gap between the energy levels are very close at high density of states and all the individual electronic states are merged to form a wide band gap above LUMO+3 levels. However, for $[\text{Zn-salen}]^{2+}$, since the orbitals are involved in bonding with the metal ion, only few independent states are appeared with small band but at high energy levels (E = 3.8 eV; LUMO +15), reducing the unoccupied electronic states. This observation is consistent with the fluorescence study that a high energy emission for the complex with respect to the ligand was observed.

With using the molecular orbitals (MOs), the hardness (η=2.43 eV) and softness (σ = 0.41 eV) were calculated [68,69] for the ligand (Fig. 10), and the values were changed to η = 1.945 and to σ = 0.51 eV after its complex with Zn^{2+}:

$$\text{Hardness}(\eta) = 1/2(E_{\text{HOMO}} - E_{\text{LUMO}}) \quad (1)$$

$$\text{Softness}(\sigma) = 1/\eta \quad (2)$$

The TD-DFT spectrum of the ligand was calculated by energy DFT at B3LYP/6-311+G(d,p) basis set with using THF as a solvent at PCM model. The calculated spectra is well comparable with the experimental spectra (See Fig 11); two absorbance peaks (λ_{exp} = 230 nm, 330 nm; λ_{calc} = 320 nm, 335 nm) attributed to $n \rightarrow \pi^*$ and $\pi \rightarrow \pi^*$ electronic transitions were observed [70]. However, there is a considerable red shift in the spectra at high energy band, consisting with the experimental spectra, where the solvent interacts significantly with the ligand, affecting the spectral band position. However, in the experimental spectrum, a weak peak appeared around 390 nm was not seen in the calculated spectra. After analyzing the previously study [47], it is seen that when some organic compounds are confined to below 50 nm (e.g. ONPs), the charge transfer phenomena becomes more dominant, thus a new peak around 400 is generated (P_{CT}) [71].

Conclusion

Organic nanoparticles (ONPs) of N,N′-ethylenebis(salicylimine) specifically recognize Zn^{2+} and Al^{3+} ions in an aqueous medium, showing that salen-ONPs performs as a chemo-sensor to detect Zn^{2+}, and also the salen-ONPs/Zn^{2+} acts as an ON–OFF switch between pH 6.0–4.0. Interestingly, the highest fluorescence intensity is seen when Al^{3+} ion is added to salen-ONPs/Zn^{2+} and it functions as a novel three inputs logic gate supported by the fluorescence for the detection of Zn^{2+} and Al^{3+}. Photo induced electron transfer (PET), which occurs in the salen-ONPs on the excitation, is inhibited when the receptor HOMO energy is lowered upon on addition of Zn^{2+} to salen-ONPs, and it enhances the fluorescence emission. This is consistent with the theoretical study that the energy of HOMO of the ligand is lower than that of Zn(salen)$^{2+}$ complex.

Acknowledgements

The authors acknowledge the Dirección General de Asuntos del Personal Académico (Project PAPIIT No IN217813) and Mexico-India-Joint Research Project [CONACYT/MEX-DST/INT] for economic support. NJ acknowledges PROMEP (IDCA 10375) for partial financial support.

Appendix A. Supplementary data

Supplementary data associated with this article can be found, in the online version, at http://dx.doi.org/10.1016/j.saa.2015.03.082.

References

[1] K. Rurack, U. Resch-Genger, Chem. Soc. Rev. 31 (2002) 116.
[2] J.J. Lavigne, E.V. Anslyn, Angew. Chem. Int. Ed. 40 (2001) 3119.
[3] V. Amendola, L. Fabbrizzi, C. Mangano, P. Pallavicini, Acc. Chem. Res. 34 (2001) 488.
[4] A.P. de Silva, D.B. Fox, A.J.M. Huxley, T.S. Moody, Coord. Chem. Rev. 205 (2000) 41.
[5] L. Fabbrizzi, M. Licchelli, P. Pallavicini, Acc. Chem. Res. 32 (1999) 846.
[6] A.W. Czarnik, Acc. Chem. Res. 27 (1994) 302.
[7] F.M. Raymo, Adv. Mater. 14 (2002) 401.
[8] F.M. Raymo, S. Giordani, J. Am. Chem. Soc. 123 (2001) 4651.
[9] F.M. Raymo, S. Giordani, J. Am. Chem. Soc. 2002 (2004) 124.
[10] V. Balzani, A. Credi, F.M. Raymo, J.F. Stoddart, Angew. Chem. Int. Ed. 39 (2000) 3349.
[11] A. Okamoto, K. Tanaka, I. Saito, J. Am. Chem. Soc. 126 (2004) 9458.
[12] D. Miyoshi, M. Inoue, N. Sugimoto, Angew. Chem. Int. Ed. 45 (2006) 7716.
[13] G. Seelig, D. Soloveichik, D.Y. Zhang, E. Winfree, Science 314 (2006) 1585.
[14] F. Xia, X.L. Zuo, R.Q. Yang, R.J. White, Y. Xiao, D. Kang, X.O. Gong, A.A. Lubin, A. Vallee-Belisle, J.D. Yuen, B.Y.B. Hsu, K.W. Plaxco, J. Am. Chem. Soc. 132 (2010) 8557.
[15] M. Zhou, Y. Du, C. Chen, B. Li, D. Wen, S. Dong, E. Wang, J. Am. Chem. Soc. 132 (2010) 2172.
[16] A.P. De Silva, H.Q.N. Gunaratne, C.P. McCoy, Nature 364 (1993) 42.
[17] A.P. de Silva, T.P. Vance, M.E.S. West, G.D. Wright, Org. Biomol. Chem. 6 (2008) 2468.
[18] F.M. Raymo, R.J. Alvarado, S. Giordani, M.A. Cejas, J. Am. Chem. Soc. 125 (2003) 2361.
[19] H. Tian, B. Qin, R.X. Yao, X.L. Zhao, S.J. Yang, Adv. Mater. 15 (2003) 2104.
[20] H.M. Wang, D.Q. Zhang, X.F. Guo, L.Y. Zhu, Z.G. Shuai, D.B. Zhu, Chem. Commun. (2004) 670.
[21] S. Uchiyama, G.D. McClean, K. Iwai, A.P. de Silva, J. Am. Chem. Soc. 127 (2005) 8920.
[22] Y. Liu, W. Jiang, H.-Y. Zhang, C.-J. Li, J. Phys. Chem. B 110 (2006) 14231.
[23] K.A. Gattas-Asfura, R.M. Leblanc, Chem. Commun. (2003) 2684.
[24] K.E. Andersen, C.Y. Fong, W.E. Pickett, J. Non-Cryst. Solids 299 (2002) 1105.
[25] A.P. Alivisatos, Science 271 (1996) 933.
[26] S.A. Empedocles, M.G. Bawendi, Science 278 (1997) 2114.
[27] L.E. Brus, J. Chem. Phys. 80 (1984) 4403.
[28] M. Bruchez, M. Moronne, P. Gin, S. Weiss, A.P. Alivisatos, Science 1998 (2013) 281.
[29] X. Michalet, F. Pinaud, T.D. Lacoste, M. Dahan, M.P. Bruchez, A.P. Alivisatos, S. Weiss, Single Mol. 2 (2001) 261.
[30] X. Michalet, F.F. Pinaud, L.A. Bentolila, J.M. Tsay, S. Doose, J.J. Li, G. Sundaresan, A.M. Wu, S.S. Gambhir, S. Weiss, Science 307 (2005) 538.
[31] M.C. Schlamp, X.G. Peng, A.P. Alivisatos, J. Appl. Phys. 82 (1997) 5837.
[32] H. Wohltjen, A.W. Snow, Anal. Chem. 70 (1998) 2856.
[33] A.N. Shipway, E. Katz, I. Willner, ChemPhysChem 1 (2000) 18.
[34] K.P. Lisha, Anshup, T. Pradeep, Gold Bull. 42 (2009) 144.
[35] N.N. Kariuki, J. Luo, L. Han, M.M. Maye, L. Moussa, M. Patterson, Y.H. Lin, M.H. Engelhard, C.J. Zhong, Electroanalysis 16 (2004) 120.
[36] D.S. Shephard, B.F.G. Johnson, J. Matters, S. Parsons, J. Chem. Soc. Dalton Trans. (1998) 2289.
[37] C.W. Corti, R.J. Holliday, D.T. Thompson, Appl. Catal. A 291 (2005) 253.
[38] M. Haruta, Gold Bull. 37 (2004) 27.
[39] J. Nam, N. Won, H. Jin, H. Chung, S. Kim, J. Am. Chem. Soc. 131 (2009) 13639.
[40] Haruta, M, Catalysis and applications of gold nanoparticles, in Science and Technology in Catalysis 2002. 2003.
[41] C.W. Corti, R.J. Holliday, D.T. Thompson, Gold Bull. 35 (2002) 111.
[42] N.D. Denkov, O.D. Velev, P.A. Kralchevsky, I.B. Ivanov, H. Yoshimura, K. Nagayama, Nature 361 (1993) 26.
[43] P. Jiang, J.F. Bertone, K.S. Hwang, V.L. Colvin, Chem. Mater. 11 (1999) 2132.
[44] E.A. Silinsh, Org. Mol. Cryst., Springer-Verlag, Berlin, 1980.
[45] H. Kasai, Y. Yoshikawa, T. Seko, S. Okada, H. Oikawa, H. Mastuda, A. Watanabe, O. Ito, H. Toyotama, H. Nakanishi, Mol. Cryst. Liq. Cryst. Sci. Technol., Sect. A 294 (1997) 173.
[46] Kasai, H, Kamatani, H, Okada, S, Oikawa, H, Matsuda, H, Nakanishi, H. Jpn. J. Appl. Phys. Part 2 1996, 35, L221.
[47] H.B. Fu, J.N. Yao, J. Am. Chem. Soc. 123 (2001) 1434.
[48] Hernández-Molina, R, Mederos, A., Acyclic and Macrocyclic Schiff Base Ligands, in: M McCleverty J.A., T.J. (Ed.), Comprehensive Coordination Chemistry II Elsevier, 2003, pp. 411.
[49] J.S. Wu, W.M. Liu, X.Q. Zhuang, F. Wang, P.F. Wang, S.L. Tao, X.H. Zhang, S.K. Wu, S. Lee, T, Org. Lett. 9 (2007) 33.
[50] X. Zhang, M. Liu, B. Yang, X. Zhang, Y. Wei, Colloids Surf., B 112 (2013) 81.
[51] X. Zhang, X. Zhang, B. Yang, M. Liu, W. Liu, Y. Chen, Y. Wei, Polym. Chem. 4 (2013) 4317.
[52] S. Li, L. He, F. Xiong, Y. Li, G. Yang, J. Phys. Chem. B 108 (2004) 10887.
[53] A.S. Nakashima, R. Dyck, H, Brain Res. Rev. 59 (2009) 347.
[54] M. El-Zein, J.L. Malo, C. Infante-Rivard, D. Gautrin, Occup. Environ. Med. 60 (2003) 655.
[55] P. Siega, R. Dreos, G. Brancatelli, E. Zangrando, C. Tavagnacco, V. Vrdoljak, T. Hrenar, Organometallics 33 (2014) 909.
[56] V. Bhalla, A. Gupta, M. Kumar, Org. Lett. 14 (2012) 3112.
[57] U.K. Mathis, M. Mohr, R. Zenobi, Atmos. Environ. 38 (2004) 4347.
[58] J.Q. Wang, L. Huang, L. Gao, J.H. Zhu, Y. Wang, X. Fan, Z. Zou, Inorg. Chem. Commun. 11 (2008) 203.
[59] deSilva, AP. Chem. Asian J. 2011, 6, 750.
[60] L.J. Liu, P. Guo, L. Chai, Q. Shi, B.H. Xu, J.P. Yuan, X.G. Wang, X.F. Shi, W.Q. Zhang, Sensors Actuators B 194 (2014) 498.
[61] D.K. Das, K. Dutta, J. Lumin. 145 (2014) 454.
[62] S. Chen, R.Q. Fan, S. Gao, X.M. Wang, Y.L. Yang, J. Lumin. 149 (2014) 75.
[63] X.R. Liang, G. Wang, Y.L. Jiang, C.L. Qu, X.J. Wang, B. Zhao, Spectrosc. Spect. Anal. 33 (2013) 3259.
[64] B.B. Ivanova, M. Spiteller, J. Incl. Phenom. Macrocycl. Chem. 75 (2013) 211.
[65] N. Jayanthi, J. Cruz, T. Pandiyan, Chem. Phys. Lett. 455 (2008) 64.
[66] Autschbach, J. Compr. Inorg. Chem. 9 (2013) 407.
[67] F. Furche, D. Rappoport, Theor. Comput. Chem. 16 (2005) 93.
[68] K. Choho, W. Langenaeker, G. VandeWoude, P. Geerlings, J. Mol. Struct. 362 (1996) 305.
[69] A.F. Jalbout, A.M. Darwish, H.Y. Alkahby, J. Mol. Struct. 585 (2002) 205.
[70] Y. Zhao, D.G. Truhlar, J. Phys. Chem. A 110 (2006) 13126.
[71] F. Wilkinson, G.P. Kelly, C. Michael, D. Oelkrug, J. Photochem. Photobiol., A 52 (1990) 309.